Research paper

Zirconia-supported tungstophosphoric heteropolyacid as heterogeneous acid catalyst for biodiesel production

Juan Alcañiz-Monge[a,*], Bouchra El Bakkali[a], Guido Trautwein[a], Santiago Reinoso[b]

[a] Departamento de Química Inorgánica, Facultad de Ciencias, Universidad de Alicante, P.O. Box 99, 03080 Alicante, Spain
[b] Institute for Advanced Materials (InaMat), Universidad Pública de Navarra (UPNA), Edificio Jerónimo de Ayanz, Campus de Arrosadia, 31006 Pamplona, Spain

ARTICLE INFO

ABSTRACT

A series of materials based on the immobilization of the 12-tungstophosphoric heteropolyacid over zirconia supports have been prepared and applied as heterogeneous acid catalysts in the esterification of palmitic acid with methanol as a model reaction for the preliminary stage of the biodiesel production. The title materials have been obtained through the sol-gel method combined with a subsequent hydrothermal treatment at mild conditions, which affords catalysts with larger porosity and higher thermal and chemical stability under the esterification reaction conditions than other preparative approaches. Generating the zirconia support by hydrolysis of an alkoxyde precursor in the presence of the heteropolyacid leads to materials with homogeneously well-dispersed clusters, as well as to an increasing contribution of the tetragonal ZrO_2 crystalline phase, a decreasing size of the nanoparticles and larger microporous volumes as the loading of the Keggin-type species increases. The 12-tungstophosphoric acid retains its catalytic activity in the esterification of palmitic acid with methanol at 60 °C upon immobilization over zirconia and conversions even higher than those observed under homogeneous conditions are obtained due to the active contribution of the support. The sample with a 30% mass percentage of heteropolyacid has been identified as the most efficient catalyst because it affords conversions above the 90% and shows the lower loss of activity over successive reaction runs among all of our materials. This loss of activity has been analyzed on the basis of the leaching of the catalyst and the fouling of the materials.

1. Introduction

Nowadays, there is a worldwide ongoing effort devoted to the development and implementation of renewable energy sources with null emissions of greenhouse gases (eg. CO_2), such as the thermosolar, photovoltaic, hydroelectric, geothermal, and wind energies. This effort includes extensive research on cleaner and more environmentally benign fuels obtained from agricultural resources, ie. biofuels [1,2]. Among liquid biofuels, biodiesel represents the green alternative to petroleum diesel because it is obtained from renewable raw materials, such as vegetable oils, fats of animal origin, or free fatty acids (FFAs) by esterification or transesterification reactions with alcohols derived from fermentation processes [3–5]. For these reactions to be of industrial interest and economic value, they are required to proceed with high conversions at mild temperatures, and these conditions can only be achieved when catalysts are introduced. A wide catalogue of compounds and materials can be used to catalyze such (trans)esterification reactions, including both basic or acid catalysts in both homogeneous or heterogeneous conditions. Among them, it is the homogeneous basic

catalysis the type of process that has been most extensively applied to date because it can afford nearly full conversions in reaction times shorter than 3 h at atmospheric pressure and temperatures as mild as 80 °C. However, this type of catalysis demands the presence of water and FFAs in the raw materials to be minimized in advance because they can lead to undesirable competing reactions, such as the formation of soaps [6], the hydrolysis of the final ester and other side reactions between the catalyst and FFAs. These competing reactions result in a decrease of the conversion and the catalyst deactivation, and therefore, they lead to a substantial increase in the purification costs due to the need of refining the raw materials prior to their use in the (trans)esterification processes [7,8]. Indeed, it is estimated that more than a half of the final cost of biodiesel originates from the need of relying on virgin or refined raw materials (eg. virgin vegetable oils) instead of using recycled wastes directly (eg. cooking oil wastes).

The costs of producing biodiesel could be reduced dramatically by designing a two-step route in which the FFAs are first esterified using an acid catalyst before proceeding into subsequent transesterification by means of basic catalysis [9,10]. The most widely used esterification acid

catalysts are common strong Brønsted acids (eg. H_2SO_4, HCl, H_3PO_4) that are inexpensive and do not lead to any saponification problems. However, they do show other significant drawbacks instead: they are environmentally unfriendly; they cause corrosion in the reactors; their reactions demand higher amounts of alcohol and catalyst (typically 5–25 wt.% for H_2SO_4, for example); and their use introduces the need of additional stages of product washing and catalyst recovery that are intrinsic to homogeneous catalytic processes. These drawbacks could be overcome by using acidic solids as heterogeneous catalysts instead of liquid mineral acids [3–5,11]. In the past few years, there has been exhaustive investigations focused on the search of new heterogeneous acid catalysts for the esterification of FFAs active enough to replicate the high conversions afforded by the homogeneous catalysis in analogous mild conditions of temperature and pressure. A plethora of acidic solids has already been explored in this context, including acidic clays [12], tantalum oxide [13], and modified zirconia [14] or silica [15]. The best results have been obtained with hydrotalcites or sulfonated zirconia, but nevertheless, the conditions to achieve suitable conversions are still far more energetic ($> 140\,°C$) than those of the homogeneous catalysis [16].

Among other suitable acidic solids, heteropolyacids (HPAs) appear as one type of candidates with the highest potential to catalyze the esterification of FFAs efficiently. HPAs are the protonated forms of the anionic metal–oxygen clusters known as polyoxometalates (POMs). POMs constitute a large family of compounds comprising species with very diverse compositions, shapes and sizes [17] where HPAs specifically refer to the subclass of heteropolyanions, which incorporate additional elements (heteroatoms) in geometrically well-defined central cavities (tetrahedral, octahedral) besides oxygen and metals from groups 5 and 6. A thorough body of reports is currently available on the catalytic applications of such POM species [18], among which $H_n[XM_{12}O_{40}]$ HPAs with the well-known Keggin-type structure constitute one the most relevant representatives ($X = $ heteroatom, e.g. Si^{IV}, P^V; $M = Mo^{VI}$, W^{VI}). HPAs behave as very strong Brønsted acids close to the super-acid region, and compared to the common mineral acids, they are significantly less harmful in terms of their environmental effects. However, HPAs show very high solubility in a range of polar solvents and this fact has led to their catalytic properties having being studied mostly in homogeneous phase. Therefore, they need to be supported on porous solid matrices for being applied under heterogeneous conditions [19–21]. Different supports have been explored to design HPA-immobilized heterogeneous acid catalysts for esterification reactions, such as mesoporous MCM-41 silica [22], zirconia [23], activated carbonaceous materials [24], or alumina [25].

Here we report our studies on the applicability of a series of HPA-immobilized porous solids as heterogeneous acid catalysts for a process of industrial and environmental relevance such as the preparation of biodiesel, and more specifically, on their performance in the preliminary stage related to the esterification of FFAs. We have chosen the palmitic acid as the FFA subject of study and its esterification with methanol into de corresponding mono-alkyl ester as the model reaction to analyze. Palmitic acid is present in significant amounts in African palm oil, the methyl ester of which displays a cetane number even higher than that of petroleum diesel, and the production of which is the highest per hectare and year among all vegetable oils originating from the cultivation of oleaginous plants, resulting in a wider availability and lower and more stable price compared to other vegetable oils for food use [26]. The combination of these features endows the biodiesel obtained from African palm oil with a high added value [27], but the significant FFA content of the raw material (ca. 5–8 wt.% of the total mass, of which the 44% corresponds to palmitic acid) hampers its widespread use by making the application of crude palm oil in a single basic transesterification stage highly inefficient. Therefore, the search for suitable heterogeneous catalysts for a preliminary acidic esterification treatment of the crude oil that eliminates the presence of FFAs (eg. palmitic acid) is of major interest. In a previous work on the application

of HPAs supported on activated carbon fibers, some of us demonstrated that the $H_3PW_{12}O_{40}$ species (hereon abbreviated as HPW) showed superior catalytic activity in the esterification of FFAs compared to other HPAs [24], and therefore, we have focused our study on this specific HPA. Zirconia (hereon abbreviated as Z) has been selected as the porous solid matrix for immobilizing the HPW catalyst, and four xHPW/Z heterogeneous catalysts with different HPA loadings ($x = $ mass percentage of HPW = 10, 20, 30 and 50 wt.%) have been prepared by a combination of the sol-gel method with a subsequent hydrothermal treatment.

2. Experimental

2.1. Materials and methods

The following materials were used for the model esterification reaction: palmitic acid, methanol and a series of supported catalysts obtained from the immobilization of $H_3PW_{12}O_{40}$ on ZrO_2. The preparation of the latter xHPW/Z catalysts involves the use of zirconium(IV) n-butoxide (80 wt.% solution in 1-butanol) and tungstophosphoric acid hydrate as reagents and ethanol as solvent. All of these materials and reagents were obtained from commercial sources (Sigma-Aldrich) and used without further purification.

The xHPW/Z catalysts ($x = $ 10, 20, 30, 50 wt.%) were prepared by the sol-gel method, followed by a hydrothermal treatment: the $Zr(n\text{-}OC_4H_9)_4$ precursor (6.0 mL, 13.0 mmol) was added to ethanol (10.0 mL, 172.0 mmol) under stirring at 60 °C. After cooling the solution down to room temperature, the pH was adjusted to a value of 2.0 with aqueous 11.6 M HCl (3.0 mL) and the corresponding amount of $H_3PW_{12}O_{40}\cdot nH_2O$ dissolved in a mixture of ethanol (12.5 mL, 214.0 mmol) and H_2O (5 mL) was added dropwise. The amounts of $H_3PW_{12}O_{40}\cdot nH_2O$ used to obtain solid materials with $x = $ 10, 20, 30 and 50% mass percentages of heteropolyacid were 0.18 g (0.06 mmol), 0.40 g (0.14 mmol), 0.69 g (0.24 mmol), and 1.60 g (0.56 mmol), respectively. It must be remarked that the amount of $Zr(n\text{-}OC_4H_9)_4$ precursor and the volume of the solution used in the preparation of the four title catalysts was the same in all cases. The resulting reaction mixture was stirred for 5 h at room temperature until a gel was formed, transferred into a Teflon autoclave, and aged for 12 h at 180 °C without stirring. The final solid material was recovered by filtration, washed several times with distilled water and dried in air for 24 h at 100 °C. The dried catalysts were characterized and used in the subsequent catalytic tests without any further calcination treatment. The pristine Z support was also obtained by following the same synthetic route applied for the preparation of the catalysts but with no heteropolyacid dissolved in the mixture of ethanol and water that is added after adjusting the pH to a value of 2.0.

2.2. Catalytic tests: esterification

The xHPW/Z solid materials ($x = $ 10, 20, 30, 50 wt.%) were evaluated as heterogeneous acid catalysts in the esterification of palmitic acid with methanol as model reaction for the preliminary stage in the preparation of biodiesel. Palmitic acid (1.0 g, 3.9 mmol) and methanol (15.0 mL, 370.0 mmol) were poured in a round-bottomed flask equipped with a reflux system and magnetic stirring. This mixture was heated to 60 °C using a thermostatic polyethylene glycol bath and the corresponding solid catalyst (0.3 g) was incorporated upon full dissolution of the palmitic acid in the alcoholic solvent. The mixture was kept at 60 °C for 6 h for the esterification reaction to proceed. Three aliquots were taken at reaction times $t = $ 1, 3 and 6 h to monitor the progress of the reaction, and more specifically, the overall yield by acid-base titration with an aqueous 0.1 M NaOH commercial standard and the nature of the reaction products by gas chromatography coupled with mass spectrometry (GC–MS). The conditions for the determination of the esterification products by GC–MS were as follows: Shimadzu

GCMS QP5050A equipped with a polydimethylsiloxane CBPI PONA-M50-042 column of dimensions 100 mm × 0.25 mm × 0.5 mm; Injection of 1 μL of a sample consisting in 1 mL of the reaction mixture diluted in 10 mL of toluene; Temperature injection: 250 °C; Split flow: 100 mL min^{-1} of He; Column flow: 1 mL min^{-1} of He; Column temperature program: 50 °C for 1 min, 10 °C min^{-1} to 200 °C, and 5 °C min^{-1} to 220 °C; Flame ionization detector (FID) temperature: 250 °C. This technique confirmed the methyl palmitate as the single reaction product. To analyze the recyclability of the heterogeneous catalysts, these were recovered by filtration after the 6 h of reaction set for the catalytic test, washed with methanol (25 mL, 60 °C, 30 min), dried in an oven at 100 °C for 12 h and reused in successive reaction cycles.

2.3. Characterization of supports and supported catalysts

The elemental analyses of the pristine Z support and of the fresh and recycled xHPW/Z catalysts are listed in Table A.1 in Appendix A of Supplementary material. The results obtained show that the elemental contents are close to the theoretical values expected for all of the zirconia-supported HPW samples. The experimental W/P ratios are in agreement with the exclusive presence of the plenary $H_3PW_{12}O_{40}$ Keggin cluster, and this fact indicates that no significant decomposition takes place either during the synthesis of the xHPW/Z materials or during the catalytic tests.

The porous texture of the pristine Z support and of the fresh and recycled xHPW/Z catalysts was characterized by physical adsorption of gases using solid samples degassed under vacuum at 100 °C for 4 h and the volumetric equipments Autosorb-B (N$_2$ at −196 °C) or Autosorb-6 (CO$_2$ at 0 °C). The specific surface area was determined from the Brunauer-Emmet-Teller (BET) equation [28] and the volume of the micropores was calculated with the Dubinin-Radushkevich (DR) equation [29]. The different pore volumes used in this work were calculated as follows [30]: a) The volume of the ultramicropores (pore size < 0.7 nm), namely V_{CO2}, was estimated from the DR curves of the CO$_2$ adsorption experiments at relative pressures $P/P_0 < 0.015$; b) The total volume of the micropores (pore size < 2 nm), namely V_{N2}, was calculated from the DR curves of the N$_2$ adsorption experiments at relative pressures $P/P_0 < 0.14$; c); The total porous volume, namely V_T, was estimated from the N$_2$ adsorption isotherm, and more specifically, from the amount adsorbed at relative pressures $P/P_0 = 0.99$; d) The mesoporous volume, namely V_{meso}, was calculated from the difference between V_T and V_{N2}.

The crystal structure of the particulate solid catalysts was examined by powder X-ray diffraction (PXRD) analyses on a Seifert JSO Debye-Flex 2002 diffractometer equipped with Cu Kα radiation. To determine whether the solid samples are chemically or structurally modified upon catalyzing the acidic esterification reaction, the fresh and recycled catalysts were studied through the following analytical techniques: diffuse reflectance infrared Fourier transform spectroscopy (DRIFTS) using a Bruker RFS/100 spectrophotometer and KBr disks as samples (10:1 wt ratio of KBr and catalyst); and thermogravimetry (TGA) using a TA Instruments SDT 2960 thermobalance equipped with a 60 cm^3 min^{-1} flow of synthetic air and a heating ramp of 20 °C min^{-1} up to 750 °C. To determine the extent of the HPW leaching upon the esterification reaction, the liquid media obtained after recovering the solid catalyst by filtration were acidified to pH 1 to ensure that all of the leached HPA is present as the fully protonated $H_3PW_{12}O_{40}$ form, and were subsequently analyzed by UV–vis spectroscopy using a Jasco UV-vis/NIR V-670 spectrophotometer. The analysis was focused on the spectral zone around 225 nm, which corresponds to the absorption maximum of the $H_3PW_{12}O_{40}$ species, and the amount of leached HPW was determined using the calibration line shown in Figure A.1 in Appendix A of Supplementary material.
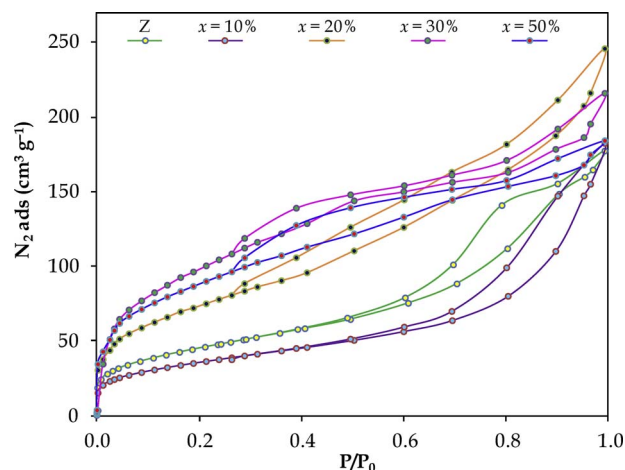

Fig. 1. N$_2$ adsorption-desorption isotherms of the xHPW/Z catalysts prepared by a combined sol-gel/hydrothermal approach with HPW mass percentages of $x = 0$ (Z support) – 50%.

3. Results and discussion

3.1. Characterization of the supported catalysts

The elemental analyses (Table A.1 in Appendix A of Supplementary material) obtained for the xHPW/Z samples show that the contents of W, P, and Zr are consistent with the theoretical values expected for all of the four zirconia-supported HPW catalysts. The experimental W/P ratios are in agreement with the exclusive presence of the plenary $H_3PW_{12}O_{40}$ Keggin cluster in our samples, and this fact indicates that no significant decomposition of the HPW species takes place during their syntheses. Moreover, the amounts of supported HPW in the four xHPW/Z samples are close to the amounts of $H_3PW_{12}O_{40}$ reagent incorporated during their syntheses as determined from the elemental composition of W and Zr, and this fact confirms that nearly the whole fraction of HPW species result embedded into the zirconia matrix by following our synthetic protocol.

3.1.1. Textural properties

Fig. 1 displays a comparison of the N$_2$ adsorption-desorption isotherms at −196 °C for the four xHPW/Z catalysts with HPW mass percentages of $x = 10, 20, 30$ and 50% that have been prepared by the sol-gel method followed by a hydrothermal treatment, as well as for the pristine Z support obtained from analogous synthetic conditions. The isotherm of the Z support is of type IV according to the IUPAC classification [31]. It shows a H2-type hysteresis loop at moderate-to-high relative pressures ($P/P_0 > 0.4$), which is characteristic of inorganic mesoporous solids, and subtle adsorption at low relative pressures ($P/P_0 < 0.2$) that associates with the presence of certain microporosity in the solid. The open shape of the isotherm elbow observed at low pressures reveals a wide distribution of micropore sizes. When the hydrolysis of the Zr^{IV} molecular source and subsequent aging stage of the resulting solid under mild hydrothermal conditions are carried out in the presence of the HPW species, the clusters result embedded in the porous Z matrix. This embedding process leads to substantial modifications of the textural properties of the final solid as shown by the significant changes in the N$_2$ adsorption-desorption isotherms of the xHPW/Z catalysts compared to that of the pristine Z support. These changes are best noticed for those samples with HPW contents equal to or higher than 20 wt.% and they mainly consist in an increase of the adsorption capacity in the lowest domain of relative pressures $P/P_0 < 0.1$, which is indicative of a relevant development of microporosity in the xHPW/Z samples.

Table 1 lists the values of the different parameters that define the textural properties of the xHPW/Z catalysts, namely the BET surface

Table 1
Textural properties of the xHPW/Z catalysts obtained from the immobilization of different mass percentages (x = 10–50%) of the $H_3PW_{12}O_{40}$ heteropolyacid over zirconia by following a combined sol-gel/hydrothermal approach.

Catalyst	S_{BET} (m^2 g^{-1})	V_{N2} (cm^3 g^{-1})	V_{CO2} (cm^3 g^{-1})	V_{meso} (cm^3 g^{-1})	V_{total} (cm^3 g^{-1})
Pristine ZrO$_2$ (Z)	164	0.08	0.05	0.17	0.27
10HPW/Z (x = 10%)	129	0.06	0.04	0.18	0.28
20HPW/Z (x = 20%)	270	0.13	0.09	0.19	0.38
30HPW/Z (x = 30%)	365	0.18	0.12	0.11	0.33
50HPW/Z (x = 50%)	321	0.16	0.11	0.09	0.28
H$_3$PW$_{12}$O$_{40}$ (HPW)	0	0	0	0	0

area (S_{BET}), the volume of the ultramicropores (V_{CO2}), the total microporous volume (V_{N2}), the mesoporous volume (V_{meso}) and the total porous volume (V_T). These values have been calculated from the N$_2$ and CO$_2$ adsorption-desorption isotherms as indicated in the Experimental Section. As shown in Table 1, the presence of low amounts of HPW (x = 10 wt.%) leads to a supported catalyst with somewhat lower microporous volume than that displayed by the pristine Z support. This fact could in principle be attributed to the "inert" weight with which the HPA clusters contribute to the solid sample upon considering the lack of porosity displayed by the commercial HPW starting material [17,18]. This subtle change in the textural properties originates exclusively from a decrease in the total microporous volume (V_{N2}) as the specific ultramicroporous (V_{CO2}) and mesoporous volumes (V_{meso}) remain nearly intact. Therefore, the immobilization of the HPW clusters must take place preferentially in the wide micropores (0.7 nm < pore size < 2.0 nm) to result in a partial block of the supermicroporosity [24], which would be in good agreement with our previous observations on HPAs being mainly adsorbed in the supermicroporous domain of activated carbonaceous supports [21]. These results are consistent with the average size of the $[XM_{12}O_{40}]^{n-}$ Keggin-type POM anions, which display diameters of 0.8–1.0 nm regardless of the addenda metal M or heteroatom X [17,32], and hence they cannot be incorporated into the ultramicropores due to size exclusion.

Higher amounts of HPW embedded into the Z support result in significantly more pronounced modifications in the porous textures of the final solid samples. When the mass percentage of immobilized HPW clusters is x = 20%, an increase of the overall microporous volume takes place, reaching values well above that of the Z support. This increase originates almost exclusively from a substantial development of the narrow microporosity, whereas the mesoporous domain is retained almost unaffected. The development of textural properties within the whole series of xHPW/Z supported catalysts reaches its maximum extent with a HPW loading of x = 30 wt.% This sample displays the highest microporous volume among all catalysts and the largest specific surface area with an S_{BET} value that more than doubles that of the pristine support. As for the 20HPW/Z sample, the increase of the microporous volume takes place mainly in the ultramicroporous domain, but in this case, this development of microporosity is accompanied by a relevant decrease of the mesoporous volume to a V_{meso} value that accounts for nearly the half of those shown by the rest of solid samples discussed above. Higher HPW loadings (x = 50 wt.%) just lead to similar slight decreases in all domains of the porosity. All of the results above indicate that the Keggin-type HPW clusters have a key role on modifying the textural properties of the Z support when the preparation of the latter via hydrolysis of zirconium(IV) n-butoxide is carried out in the presence of HPW amounts up to x = 30 wt.%, whereas higher amounts of the HPA species do not influence the development of the porous structure of the resulting solid in a significant manner. It should be noted at this point that the HPW:ZrO$_2$ molar ratio ranges from 0.005 in 10HPW/Z to 0.040 in the sample with the highest HPW loading (50HPW/Z), and hence our immobilized catalysts contain a very low number of POM cluster units per Zr site that, nevertheless, are able to promote noticeable modifications in the textural properties of the support.

The preparation of our xHPW/Z samples through the entrapment of different amounts of the $H_3PW_{12}O_{40}$ acid catalyst into a ZrO$_2$ matrix formed in situ from the hydrolysis of zirconium(IV) n-butoxide via the sol-gel method followed by hydrothermal aging is not a fully unprecedented synthetic route for the heterogenization of HPAs in inorganic oxide supports. For example, the HPW species has been previously immobilized in ZrO$_2$ using the sol-gel method to prepare photocatalysts for the selective aerobic oxidation of alcohols [33], but in this case, the POM-loaded gel was calcined at high temperatures to fasten the zirconia network instead of being hydrothermally treated at milder conditions. Hydrothermal conditions to age POM-loaded hydrogels into inorganic oxides have been applied by Wang and coworkers to obtain a TiO$_2$-supported HPW photocatalyst for the degradation of dye pollutants [34]. During the hydrolysis of the Zr^{IV} molecular precursor, the Keggin-type HPW units result embedded into the Zr(OH)$_4$ hydrogel as it forms, in such a way that the clusters result immobilized in the final hydrothermally-generated ZrO$_2$ matrix through both electrostatic interactions and the formation of extensive hydrogen-bonding. The ≡Zr−OH groups of the zirconia protonate into ≡Zr−OH$_2$$^+$ due to the acidic environment provided by the HPA species, resulting in the formation of electrostatic $[≡Zr−OH_2]^+[H_2PW_{12}O_{40}]^-$ pairs through an acid-base-like reaction [33,34]. Moreover, these interactions are reinforced by the massive ≡Zr−OH···O$_t$ = W and ≡Zr−OH···O$_b$ = W hydrogen bonding interactions that the surface oxido ligands O$_t$ (terminal oxygen atom) and O$_b$ (bridging oxygen atom) of the POM clusters can establish with the ≡Zr−OH groups of the zirconia network. Taking into account the diameter of ca. 0.8 nm displayed by the Keggin clusters, this mechanism for the anchoring of the HPW units would support the modifications observed for the textural properties of our samples as the largest development of porosity takes place in the microporous structure, and more specifically, in the domain of the pores with sizes equal to or lower than 0.8 nm. Considering that the Keggin-type units are immobilized onto the surface of the zirconia nanoparticles through the interactions discussed above, it is likely that an increasing number of individual clusters result trapped in between adjacent nanoparticles as higher amounts of HPW are loaded. Two adjacent nanoparticles sandwiching a Keggin unit would then be separated by a distance analogous to the diameter of the cluster, leading to the generation of interparticle void spaces that would lie in the ultramicroporous domain.

3.1.2. Powder X-ray diffraction

Fig. 2 shows the PXRD patterns of the whole series of xHPW/Z samples (x = 10–50 wt.%) compared with those of the commercial HPW starting material and the pristine Z support obtained by following the synthetic route applied for the preparation of the catalysts. It is worth noting first the presence of broad but well-defined diffraction maxima in the pattern of the pristine Z support isolated from the hydrolysis of the zirconium(IV) n-butoxide molecular precursor and subsequent hydrothermal treatment at 180 °C. This relatively crystalline character of the solid contrasts with the mainly amorphous nature of zirconia samples prepared by following precipitation synthetic approaches or pure sol-gel routes without any hydrothermal aging stage, the PXRD patterns of which do not show any defined diffraction
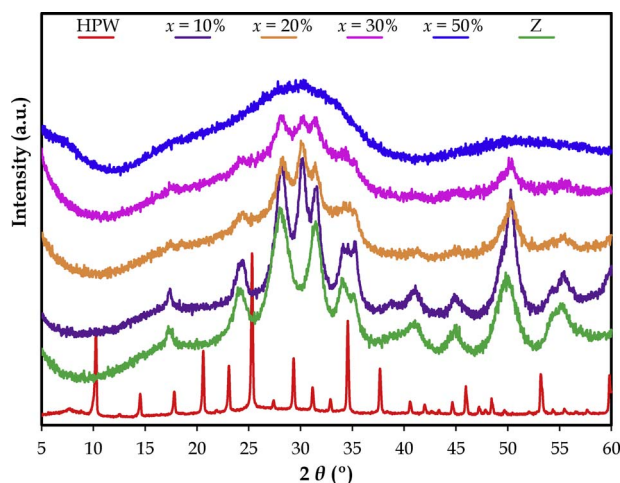
Fig. 2. Powder X-ray diffraction patterns of the xHPW/Z supported catalysts prepared by a combined sol-gel/hydrothermal method with HPW mass loadings in the $x = 0$ (Z support) – 50 wt.% range.

Fig. 3. DRIFT spectra of the xHPW/Z catalysts prepared by a combined sol-gel/hydrothermal method with HPW mass loadings in the $x = 0$ (Z support)– 50 wt.% range. The arrows highlight those signals that undergo an increase in intensity with increasing the HPW loading.

maxima. Therefore, these hydrothermal aging conditions applied on the as-hydrolyzed zirconia have proven to be effective for developing certain crystallinity in the final solid samples at relatively low temperatures, which is consistent with literature reports on some other inorganic oxides such as zeolites or cordierites [35]. The main diffraction maxima appear at 2θ ca. 24, 28, 32, 42, 46, 54 and 56° and they correspond to the monoclinic phase of zirconia [36], but a minor contribution of the tetragonal phase can also be observed with its diffraction maxima located at 2θ ca. 30, 35 and 50° [37].

Loading the zirconia with low quantities of the HPW species enhances the crystallinity of the Z support as indicated by the sharper and more intense diffraction maxima observed in the pattern of the 10HPW/Z sample. Thus, the acidic forms derived from Keggin-type clusters appear to behave as mineralizing agents in the wet-synthesis of inorganic oxides when they are present in the reaction medium in such small amounts ($x = 10$ wt.%), in close analogy to the role played by other mineral acids in the hydrothermal synthesis of zeolites [38]. Under these conditions, the HPW species in our 10 HPW/Z sample does not only lead to an improved crystallinity, but it also promotes an increase of the particle size and a modification of the crystallographic ordering. The application of the Scherrer equation to the diffraction maxima located at 2θ ca. 28 and 50° reveals that the average size of the zirconia nanoparticles more than doubles when going from the pristine Z support (ca. 4 nm) to the 10HPW/Z sample (ca. 9 nm), and at the same time, that the contribution of the tetragonal fraction to the mixture of crystalline phases notably increases (note the resolution of a new diffraction maximum at ca. 30° in the pattern of 10HPW/Z), although not enough for becoming the major component. In contrast, higher HPW loadings result in a continuing amorphization of the solid material. The pattern of the 20HPW/Z sample with just an HPW loading of $x = 20$ wt.% already shows a substantial loss of crystallinity based on the noticeable broadening and decrease of intensity of the diffraction maxima, which continue to fade away in the pattern of the 30HPW/Z solid and become fully unresolved in that of the nearly amorphous 50HPW/Z material with the highest mass percentage of HPW ($x = 50$ wt.%). It is worth mentioning that no sign of the characteristic pattern of the commercial HPW starting material [39] is observed for any of our xHPW/Z catalysts, not even for the 50HPW/Z material, which indicates that the HPW particles are most likely very small in size and homogeneously dispersed into the pores of the Z support in good agreement with the immobilization mechanism discussed above.

The experimental results obtained from the PXRD measurements are consistent with the modifications observed in the textural properties throughout the whole series of xHPW/Z catalysts. On the one hand, the
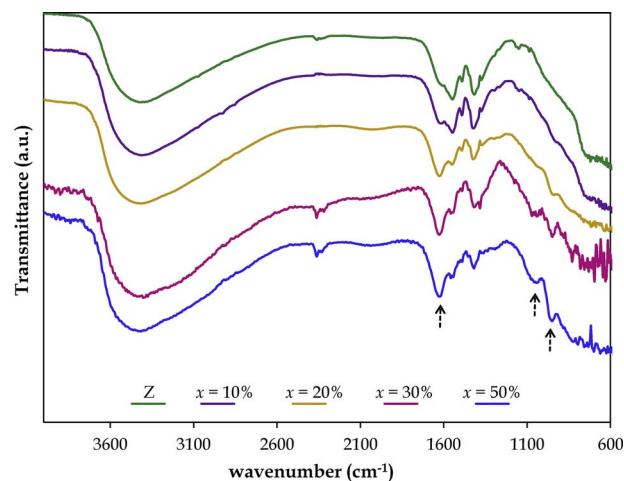
modifications undergone by the porous texture of the pristine Z support when loaded with the lowest amount of HPW (10HPW/Z sample) were barely noticeable, and so are the differences between their corresponding PXRD patterns but for an enhancement of the crystallinity. On the other hand, the mesoporous volume of those catalysts with the highest HPW loadings (30HPW/Z and 50HPW/Z samples) dropped to values that are nearly the half of that of the Z support and this fact is consistent with the significant decrease of the average size undergone by their constituent zirconia nanoparticles as indicated by the fact that the diffraction maxima progressively go from well-defined peaks to broader bands until they lose all resolution. Therefore, it is plausible that the presence of high amounts of HPW during the hydrothermal treatment of the $Zr(OH)_4$ hydrogel hinders the growth of large ZrO_2 nanoparticles, the interparticle space among which generates the mesoporosity of the materials, but brings together the resulting small particles to distances around the diameter of a Keggin cluster facilitating the development of narrow microporosity instead.

3.1.3. Diffuse reflectance infrared Fourier transform spectroscopy

Fig. 3 shows the DRIFTS spectra of the pristine Z support compared with those of the whole series of xHPW/Z supported catalysts with HPW loadings in the range $x = 10$–50 wt.% The spectrum of the Z support obtained from the combined sol-gel/hydrothermal synthetic approach is similar to those of zirconia samples prepared by following precipitation or pure sol-gel methods [40]. As main features, this spectrum displays a broad band of absorption in the 2500–3700 cm^{-1} range originating from the stretching O−H vibration of the surface $\equiv Zr-OH$ groups, a band of absorption in the $1500-1700$ cm^{-1} domain that associates with bending vibrations in the physisorbed water molecules, and a second broad band of absorption centered at ca. 820 cm^{-1} that corresponds to the stretching vibration of the Zr−O bonds [41]. However, some differences can be found in the 1220–1460 cm^{-1} range when comparing the spectrum of our Z support with the other zirconia samples prepared by alternative routes [40]. In the latter, an absorption band centered at 1350 cm^{-1} that corresponds to bending vibrations of crystallization water molecules can be observed [42]. In our case, this signal appears as a weak shoulder shadowed by an absorption band of much stronger intensity that is centered at ca. 1420 cm^{-1}. This absorption band could tentatively be assigned to bending H−C−H vibrations of the methyl (–CH$_3$) and methylene (–CH$_2$–) groups of n-butoxide anions belonging to small amounts of the Zr^{IV} molecular precursor that have been left unreacted. The incorporation of the HPW species into the Z support induces

progressive variations in the DRIFT spectra as the HPW loading goes from 10 to 50 wt.% The absorption bands in the 1500–1700 and 1220–1460 cm^{-1} ranges become increasingly weaker and this fact indicates a more efficient transformation of the molecular precursor into zirconia, as well as a lower content of physisorbed water molecules due to the clusters occupying the micropores and the partial collapse of the mesoporous structure for those samples with the highest HPW loadings. In contrast, a new signal of increasing intensity throughout the series of xHPW/Z catalysts appears at ca. 1620 cm^{-1}. As for the previous absorption band in the 1500–1700 cm^{-1} range, this new signal also corresponds to bending vibrations of water molecules, but in this case, these molecules can be assigned as $H_5O_2^+$ ions belonging to the secondary structure of the hydrated HPW species rather than being merely physisorbed, the peak at 1620 cm^{-1} originating from the in-plane bending vibration of the H−O−H bridge [43,44]. The characteristic fingerprint of the primary structure of the 12-tungstophosphoric Keggin-type cluster can be barely noticed [45], not even for the 50HPW/Z sample with the highest HPW loading. This fact is consistent with the immobilization mechanism discussed above, which results in a homogeneous, fine dispersion of HPW species over the surface of the nanoparticles that constitute the zirconia matrix. Nevertheless, the presence of HPW units in our samples can be addressed from two peaks of increasing intensity with the HPW loading. These absorption bands appear at ca. 1060 and 980 cm^{-1} and originate from the antisymmetric stretching vibrations of the P−O bonds in the central heterogroup of the cluster and the surface W = O$_t$ bonds involving terminal oxo ligands, respectively.

3.1.4. Thermogravimetric analyses

The thermogravimetric curves of the pristine Z support and the whole series of xHPW/Z supported catalysts prepared in this work are displayed in Fig. 4. The support obtained from the combined sol-gel/ hydrothermal synthetic approach shows higher thermal stability than other zirconia samples prepared following the more usual precipitation or pure sol-gel methods [40]. Our support undergoes a mass loss of only 3% up to 300 °C, which contrasts with the mass losses well-above 10% and up to 20% displayed in this temperature range by the zirconia samples obtained from other alternative synthetic routes [40]. This observation strongly suggests that the hydrothermal conditions applied in our work induce more efficient hydrolysis and condensation reactions of the Zr^{IV} molecular precursor, as well as better dealcoholation of the alkoxide anions from the resulting Zr(OH)$_4$ hydrogel, which would result in a final solid with a lower content of physisorbed water molecules and surface ≡Zr−OH groups, hence with lower content of mass that can be thermally evacuated. Furthermore, a better efficiency of the

Fig. 4. Thermogravimetric curves of the xHPW/Z solid catalysts with HPW mass loadings in the x = 0 (Z support) – 50 wt.% range.

hydrolysis-condensation processes would also be consistent with the crystalline nature displayed by our support in contrast to the amorphous character of the zirconia obtained from other preparative methods [40].

In regard to the mass losses, the first stage up to ca. 200 °C corresponds to the evacuation of the physisorbed water, and most likely, of some ethanol used as solvent in the synthetic procedure also. The second stage up to ca. 300 °C originates from the release of the residual organic matter, and more specifically, of the minor fraction of n-butoxide anions that could remain in the sample upon dealcoholation of the Zr(OH)$_4$ hydrogel [33]. The mass loss that takes place in the temperature range from 300 to ca. 500 °C relates to the transformation of residual Zr(OH)$_4$ into ZrO$_2$, which involves the release of some structural water molecules as a result of the loss of terminal hydroxyl groups during the formation of the zirconia lattice [46], whereas the last mass loss stage from ca. 570–700 °C associates with the combustion of that organic matter that could remain occluded within the solid upon formation of the zirconia.

Loading the zirconia with low quantities of the HPW species (10HPW/Z sample) leads to a thermogravimetric curve with a shape virtually identical to that of the Z support alone. The overall mass loss substantially decreases due to a somewhat lower content of physisorbed water molecules as a result of the clusters blocking part of the supermicroporous structure, but mainly, to a much lower extent of the transformation of residual Zr(OH)$_4$ into ZrO$_2$ that takes place in the 300–500 °C range. The latter observation is consistent with the higher degree of crystallinity showed by the 10HPW/Z sample when compared to the pristine Z support. In contrast, the incorporation of higher amounts of HPW results in significant modifications of the thermogravimetric curves, which mainly consist in a noticeable development of the mass loss stage up to 200 °C associated with the progressive fading of that corresponding to the 300–500 °C range. The development of the former stage originates from an increasing amount of water molecules clustered around the secondary structure of the hydrated HPW species as $H_5O_2^+$ ions, whereas the fading of the latter stage relates to the decrease of free ≡Zr−OH groups as an increasing number of HPW clusters get immobilized at the surface of the zirconia nanoparticles through a mechanism of acid-base proton exchange. Finally, it must be pointed out that the primary structure of the Keggin-type HPW cluster is thermally robust and remains intact until ca. 500 °C before proceeding into its breakdown into the corresponding oxides [42].

3.2. Evaluation of the catalytic activity

The four xHPW/Z materials prepared in this work with HPW mass percentages of x = 10, 20, 30, and 50% were evaluated as supported acidic catalysts in the esterification of palmitic acid with methanol at 60 °C as a model reaction for the preliminary stage of esterification of FFAs in the preparation of biodiesel. The catalysts were used as-isolated without any previous calcination treatment because any thermal treatment above 150 °C lowers the number of $H_5O_2^+$ ions in the secondary structure of the Keggin-type clusters, and hence the acidity of the hydrated HPW species as illustrated by the thermal evolution of the DRIFT spectra of the 30 HPW/Z sample that is displayed in Figure A.2 . in Appendix A of Supplementary material. In addition, an important decrease in the porosity also takes place when the samples are calcined at temperatures above 100 °C as shown in Figure A.3 in Appendix A of Supplementary material. To exemplify the comments above, Figure A.4 in Appendix A of Supplementary material shows how the conversions achieved with the 50 HPW/Z sample get systematically lower as the catalyst is calcined at increasing temperatures. Fig. 5 shows the conversions achieved with the different quantities of supported HPW catalyst present in 0.3 g of the title xHPW/Z materials and a comparison with the conversions provided by the same amounts of commercial HPW starting material.

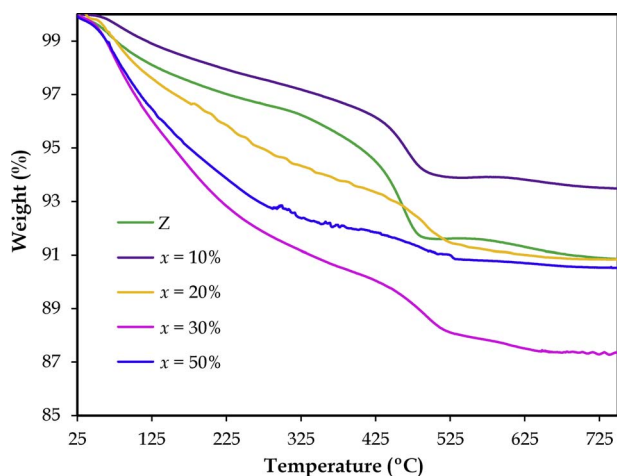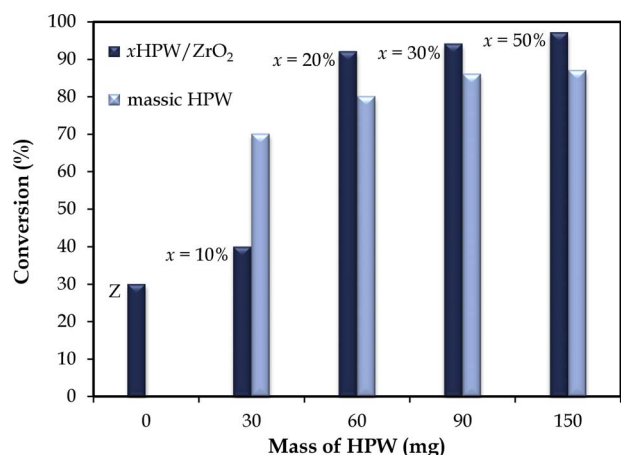The commercial HPW is soluble in the reaction medium (methanol),

Fig. 5. Conversion of palmitic acid upon esterification with methanol for 6 h at 60 °C as a function of the amount of HPW acid catalyst (commercial or immobilized on the ZrO$_2$ support).

Fig. 6. Conversion of palmitic acid into methyl palmitate over five consecutive esterification cycles with methanol (each running for 6 h at 60 °C) using 0.3 g of xHPW/Z catalysts (x = 20, 30 or 50 wt.%).

and therefore, it acts as a homogeneous acid catalyst in the esterification of palmitic acid. This HPA species already affords high conversions of nearly the 70% with just 10 μmols (30 mg) added to the reaction mixture. The conversion is maximized to a value around the 85% when 90 mg of the HPW catalyst are used [24]. Upon immobilization at the zirconia generated by the combined sol-gel/hydrothermal preparative approach, the HPW species retains its catalytic activity in the title esterification reaction and shows similar trends to those observed when used in the homogeneous phase, that is, the conversion rises with the amount of catalyst to reach optimized values for 60–90 mg of HPW and remains mostly unaffected by further increases in the amount of added catalyst. The fact that our zirconia-supported acid catalysts display similar activity in the esterification of palmitic acid than that observed in homogeneous conditions is noteworthy and contrasts with the results included in a number of literature reports, which evidence that HPAs partially lose their activity as acid catalysts upon heterogenization [47,48]. In our case, the xHPW/Z materials with HPW loadings above the 10 wt.% show even higher activity than the unsupported HPW catalyst and conversions of almost the 95% are reached when the 30HPW/Z sample (90 mg of HPW) is used. This behavior can be traced back to the influence of the zirconia matrix in the catalytic properties of the xHPW/Z materials because our pristine Z support prepared under analogous synthetic conditions is also able to catalyze the esterification reaction to some extent, leading to conversions of ca. 30%. This fact can be attributed to the existence of Brønsted acidic sites at the surface of our zirconia as a result of the hydrochloric acid used to set the pH conditions at which the support is synthesized, and resembles the properties shown by ZrO$_2$ materials modified with sulfuric acid, which are used as acid catalysts for manifold organic reactions including the esterification of FFAs [49–51].

The high catalytic activity shown by the zirconia-supported HPW species evidences the facile accessibility of palmitic acid toward the active sites in the constituent nanoparticles of the Z support. Taking into account the large dimensions of the substrate with a linear alkyl chain of 16 carbon atoms and a carboxylic head (1.9 nm length × 0.6 nm diameter), the ease with which the palmitic acid reaches the active sites of the catalyst would not be a priori expected if the latter were only located within the microporous structure with pore sizes lower than 2 nm. Therefore, the results obtained for the catalytic activity of the xHPW/Z materials further supports the model proposed for the anchoring of the clusters at the surface of the zirconia nanoparticles, which would render much more accessible HPW species.
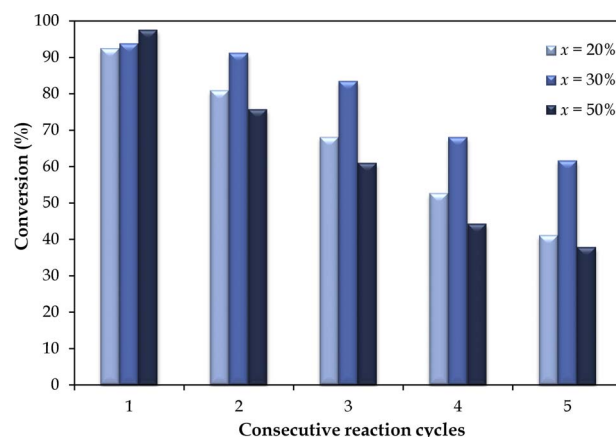
3.3. Evaluation of the recyclability of the supported catalysts

A key feature of heterogeneous catalysts resides in their ability of being reused in successive reaction cycles without substantial loss of their properties. The recyclability of a given heterogeneous catalyst is of great relevance not only from an economic viewpoint, but also because of operational aspects related to the charge and discharge of the reactors [52]. In most cases, the recycling of a supported catalyst demands a preliminary stage of regeneration of the active phase before being reused in a new reaction run. In our case, however, the recyclability of those xHPW/Z materials with the highest catalytic activity (x = 20, 30 and 50 wt.%) was evaluated by applying the supported catalysts in successive esterification runs without any intermediate regeneration stage. The conversions afforded by these materials throughout five consecutive reaction cycles are shown in Fig. 6. For all xHPW/Z materials, the activity decreases with each reaction run but the magnitude of this decrease is dependent on the HPW loading. For example, the 50HPW/Z sample shows the highest initial activity but its loss throughout the five esterification cycles is the more pronounced among all tested samples, resulting in the less efficient catalyst despite containing the largest amount of catalytically active HPW species. The relative loss of activity in the fifth consecutive run with regard to the first cycle has been calculated to the following values: 51% for 20HPW/Z, 33% for 30HPW/Z and 59% for 50HPW/Z. Therefore, the 30HPW/Z sample appears as the most suitable recyclable catalyst for the selected model reaction.

3.3.1. Leaching of the active catalyst

Another key feature of heterogenized catalysts is the leaching of the supported active species toward the reaction medium, which results in a sequential loss of catalytic activity throughout successive reaction cycles and the potential contamination of the reaction products. This process is particularly common for supported catalysts based on POM clusters and it has been previously described for several materials that contain the HPW species immobilized on different solid matrices, and that operate under reaction conditions analogous to those of our model esterification reaction [22–24]. To quantify the amount of leached HPW species from our xHPW/Z materials during five consecutive esterification cycles, the solutions obtained upon filtration of the solid catalyst out from the reaction media were analyzed by UV–vis spectroscopy after each reaction run was completed. In addition, elemental analyses were also performed on the recycled catalyst samples (Table A.1 in Appendix A of Supplementary material). Fig. 7 shows a comparison of the spectra obtained for the most efficient catalyst among the title materials, namely 30HPW/Z, whereas those corresponding to the 20HPW/Z and 50HPW/Z samples are displayed in Appendix A of
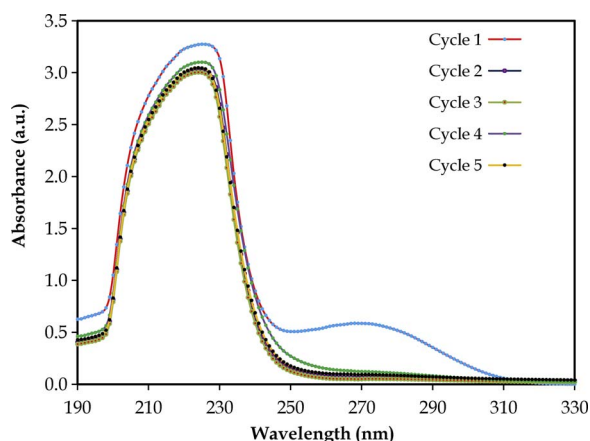
Fig. 7. UV–vis spectra of the reaction medium corresponding to the esterification of palmitic acid with methanol catalyzed by 0.3 g of the 30HPW/Z sample recorded throughout five consecutive cycles, each cycle running for 6 h at 60 °C.

Supplementary material (Figures A.5 and A.6, respectively).

For the 30HPW/Z material, the UV–vis spectra of the liquid media after completion of each reaction cycle showed all an absorption band of strong intensity located around 225 nm. This absorption band corresponds to the absorption maximum of the Keggin-type $[PW_{12}O_{40}]^{3-}$ POM and evidences that part of the catalytically active HPW species leaches from the Z support during the esterification process. Moreover, these absorption bands compare very nicely in terms of shape and intensity in all of the spectra, which reveals that the amount of leached HPW must be similar for each of the reaction runs. These amounts have been quantified using the calibration line provided in Figure A.1 in Appendix A of Supplementary material, and the results, together with those corresponding to the 20HPW/Z and 50HPW/Z samples, are listed in Table 2 on the basis of the initial mass percentages of HPW present in the fresh catalysts, which have been obtained from elemental analyses (Table A.1 in Appendix A of Supplementary material). In general, the amount of leached HPW species is very low for all samples and decreases with increasing the initial HPW loading. Moreover, the amount of leached catalyst is very similar for each of the five consecutive reaction runs not only in the case of the 30HPW/Z sample, but also for the material with an initial mass percentage of HPW of $x = 20\%$. Only in the case of the sample with the highest initial HPW loading (50HPW/Z), a progressive decrease of the amount of leached catalyst is observed as more reaction cycles are cumulated. The relatively low values listed in Table 2 contrast with those reported for other materials obtained from the immobilization of the HPW species on different solid supports, such as activated carbon fibers or mesoporous MCM-41 silica, for which the percentage of leached catalyst has been calculated to be as high as the 40 and the 20%, respectively [24,53]. These results highlight the suitability of the synthetic protocol followed in this work to immobilize the HPW species over the zirconia support, which leads to strongly anchored POM clusters and hinders significant leaching of the catalytically active species under the reaction conditions applied for esterifying palmitic acid with methanol.

Close inspection of the data listed in Table 2 also reveals another two relevant aspects. First, the amount of HPW that is transferred from the xHPW/Z materials into the liquid reaction medium for each

reaction cycle must range from 3 to 4 mg, and according to the results shown in Fig. 5, such low quantities can only lead to a maximum conversion of approximately the 30% upon considering that all of the leached HPW acts as a homogeneous catalyst during the full reaction run of 6 h. Therefore, our results confirm that the esterification of palmitic acid into methyl palmitate proceeds mainly in the heterogeneous phase when catalyzed by our xHPW/Z materials. Second, the amount of HPW that remains immobilized on the zirconia support after the fifth reaction cycle as estimated from the UV–vis calibration curve (Figure A.1 in Appendix A of Supplementary material) is consistent with that determined from the elemental analyses performed on the recycled catalysts (Table A.1). For example, the HPW supported on 0.3 g of catalyst after five cycles is 84 mg for the 30HPW/Z sample and 144 mg for the 50HPW/Z sample, and according to the results displayed in Fig. 5, such HPW loadings should be more than enough to reach conversions higher than the 80% under our reactions conditions. Therefore, the significant decrease of the catalytic activity shown by these xHPW/Z materials over the five consecutive esterification cycles must be mainly attributed to factors other than the HPW leaching.

3.3.2. Fouling of the supported catalysts

A third key feature that can hamper heterogeneous catalysts from being reused in consecutive reaction cycles is related to the inaccessibility of the reagents toward the active sites present within the porous structure due to the fouling of the catalyst. Palmitic acid is a solid with a relatively low melting point (62.9 °C), with a boiling point of 351 °C, immiscible with water, poorly soluble in cold methanol and relatively soluble in hot methanol. All of these characteristics suggest that palmitic acid should easily solidify under our reaction conditions because the esterification process is carried out using a solvent in which dissolves poorly and a temperature below its melting point. Therefore, the fact that fractions of palmitic acid or its esterification product methyl palmitate could become retained and cumulated within the porous structure of the zirconia support after each reaction cycle, thus progressively blocking the accessibility toward the active HPW species, appears as a reasonable hypothesis to explain the decrease of the catalytic activity observed for the title xHPW/Z materials. This phenomenon has been previously described in the literature for both supported catalysts based on immobilized HPW and other types of heterogeneous catalysts [24,54]. To explore whether our xHPW/Z materials get fouled during the esterification process, we performed thermogravimetric analyses on those samples with HPW loadings of $x = 20$, 30 and 50 wt. % that were recovered by filtration after the fifth reaction run (hereon noted as xHPW/Z-C5) and compared the results with the thermogravimetric curves of the corresponding fresh catalysts (Fig. 8 and
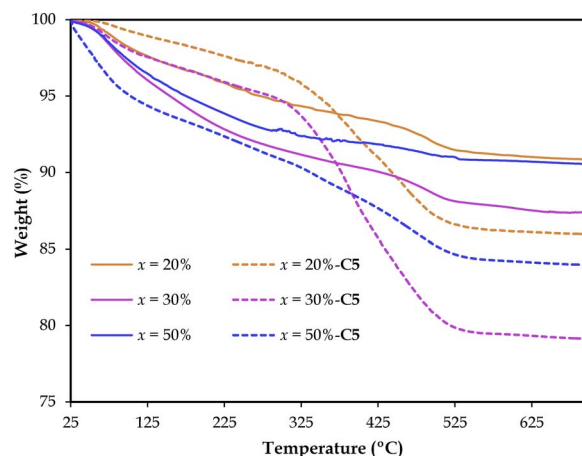

Fig. 8. Thermogravimetric curves of the fresh xHPW/Z catalysts ($x = 20$, 30, and 50 wt. %) compared to those of the recycled catalysts after 5 consecutive six-hours-long esterification runs of palmitic acid with methanol at 60 °C (xHPW/Z-**C5**).

Table 2
Mass percentage (%) of the leached HPW heteropolyacid over five consecutive esterification cycles based on the initial amount of HPW present in the fresh xHPW/Z catalysts.

Catalyst	Cycle 1	Cycle 2	Cycle 3	Cycle 4	Cycle 5
20HPW/Z	6.6	6.5	6.7	6.5	6.6
30HPW/Z	4.2	3.8	3.7	3.9	3.8
50HPW/Z	3.2	2.5	2.1	1.9	1.8

Table 3
Total mass losses (%) at 600 °C for fresh (xHPW/Z) and recycled catalysts after five consecutive esterification cycles (xHPW/Z-C5).

Fresh catalyst	Mass loss (%)	Recycled catalyst	Mass loss (%)
20HPW/Z	9	20HPW/Z-C5	14
30HPW/Z	12	20HPW/Z-C5	21
50HPW/Z	11	50HPW/Z-C5	16

Table 4
Comparison between the textural properties of the fresh (xHPW/Z) and recycled catalysts after five consecutive reaction cycles (xHPW/Z-C5).

Catalyst	S_{BET} ($m^2 g^{-1}$)	V_{N2} ($cm^3 g^{-1}$)	V_{CO2} ($cm^3 g^{-1}$)	V_{meso} ($cm^3 g^{-1}$)	V_{total} ($cm^3 g^{-1}$)
20HPW/Z	270	0.13	0.09	0.19	0.38
20HPW/Z-C5	148	0.07	0.04	0.15	0.25
30HPW/Z	365	0.18	0.12	0.11	0.33
30HPW/Z-C5	78	0.04	0.05	0.08	0.14
50HPW/Z	321	0.16	0.11	0.09	0.28
50HPW/Z-C5	99	0.05	0.04	0.03	0.09

Table 3). In addition, elemental analyses have also been performed on these recycled xHPW/Z-C5) samples (Table A.1 in Appendix A of Supplementary material).

In all cases, the recycled catalysts undergo higher mass losses upon heating than those observed for the fresh materials, which according to the thermogravimetric curves, originate from additional mass loss stages that appear in the temperature range from ca. 300–500 °C. Therefore, the recycled catalysts do retain a certain amount of additional matter that undergoes thermal desorption at temperatures higher than those corresponding to the mere evacuation of physisorbed solvent molecules, and therefore, most likely corresponds to organic matter belonging to the palmitic acid reagent and/or the methyl palmitate product. The elemental analyses of the recycled catalysts (Table A.1 in Appendix A of Supplementary material) confirm this observation because a significant amount of C was detected on the xHPW/Z-C5 samples (6.8 wt.% and 8.3 wt.% for the 50HPW/Z-C5 and 30HPW/Z-C5 samples, respectively). In regard to the amount of retained matter, the results above allow for correlating the decrease of activity of our xHPW/Z materials over consecutive esterification cycles with a fouling effect by accumulation of matter at the catalytically active sites, but the fact that the largest amount of cumulated matter after five reaction runs corresponds to that sample for which the smoothest decrease of activity has been observed (30HPW/Z) is surprisingly noteworthy.

The nature of the species adsorbed in the used catalysts has been explored by DRIFT spectroscopy. As an illustrative example, Fig. 9 displays a comparison between the spectrum of the fresh 30HPW/Z material with that of the same sample after catalyzing one esterification cycle. The spectrum of the latter shows two additional peaks of weak-to-medium intensity located at 2925 and 2855 cm^{-1}, which are characteristic of long alkyl chains such as that of the palmitate molecule and originate from the stretching C—H vibrations in the terminal methyl and middle methylene groups. This observation confirms that the retained matter is organic and corresponds to palmitate from the acidic reagent and/or the esterified product. To evaluate whether the retention of fouling matter is merely superficial or takes place within the porous structure of the catalysts, the textural properties of the recycled xHPW/Z-C5 materials were analyzed through comparison of their N_2
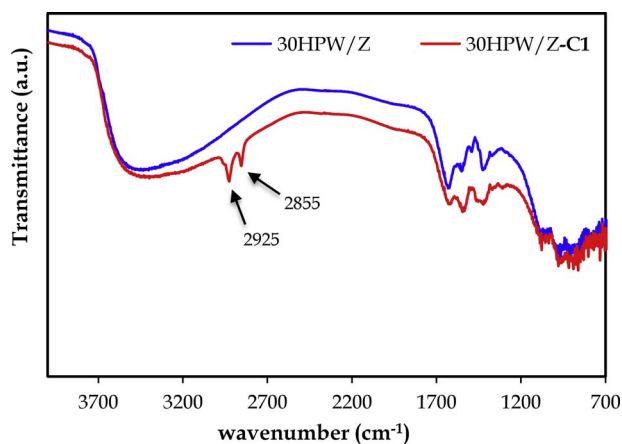
and CO_2 adsorption-desorption isotherms with those of their corresponding freshly prepared xHPW/Z samples. The results obtained from this comparison are listed in Table 4 and reveal that the volumes of all kinds of porosity decrease after catalyzing the five consecutive esterification runs, but this decrease follow different trends in each of the samples and for each specific type of pore. In general, the mesoporosity is the class of porous volume that varies the less, whereas the most pronounced modifications are observed for the total microporosity, which can be clearly noticed in the great shift toward lower values of adsorbed N_2 that the isotherms displayed in Fig. 10 undergo in the range of relative pressures lower than 0.3. These results confirm that the porous structure of the xHPW/Z materials result partially filled with the palmitate-based molecules upon catalyzing the esterification reaction and they indicate that the accumulation of these molecules takes place preferentially in the micropores. This observation is reasonable as the adsorption potential in this class of porosity is usually higher than that displayed by the mesopores. In regard to the catalysts, the 20HPW/Z material is the sample for which the microporous volume decreases the less, whereas 30HPW/Z constitutes the material showing the largest modification in its microporosity. These results are fully consistent with the amounts of retained organic matter determined by thermogravimetric analyses (Table 3).

4. Conclusions

The preparation of heterogeneous catalysts based on zirconia-supported 12-tungstophosphoric acid through the sol-gel method combined with a subsequent hydrothermal treatment at mild conditions has proven to result in a more efficient method for the immobilization of Keggin-type heteropolyacids than other preparative routes, such as the pure sol-gel or the precipitation methods. Our combined synthetic approach affords materials with larger porosity and higher thermal and
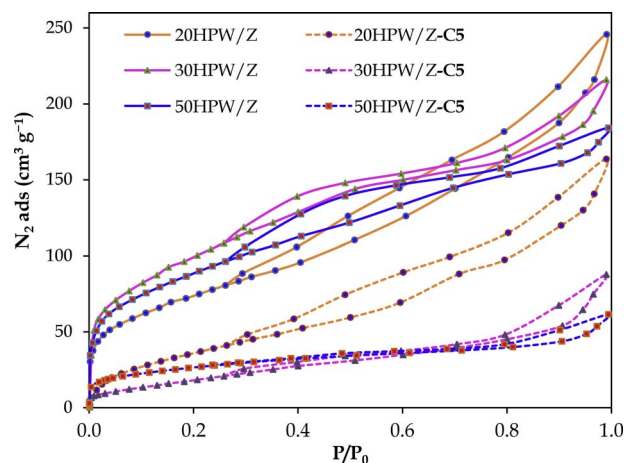

Fig. 9. Comparison between the DRIFT spectrum of the fresh 30HPW/Z sample and that of the same catalyst after performing one esterification cycle (30HPW/Z-C1).

Fig. 10. Adsorption-desorption N_2 isotherms of the fresh 20-, 30- and 50HPW/Z samples compared to those of the same materials after catalyzing five consecutive esterification cycles (xHPW/Z-C5).

chemical stability under the esterification reaction conditions. The synthesis of the zirconia support in the presence of the heteropolyacid leads to significant modifications in both the composition and the morphology of the resulting material. Increasing the loading of heteropolyacid induces variations in the crystallographic ordering of the zirconia, which consist in a progressive development of the minor tetragonal fraction within the mixture of crystalline phases and the decrease of the average size of the zirconia nanoparticles. Moreover, higher loadings of heteropolyacid also result in larger microporous volumes, mainly due to the development of the ultramicroporous structure to larger extents. The results obtained from the powder X-ray diffraction and diffuse reflectance infrared Fourier transform analyses indicate that the polyoxometalate clusters disperse homogeneously over the support regardless of the amount of heteropolyacid immobilized over the zirconia as the characteristic signals of Keggin-type clusters are hardly detected by these techniques.

The 12-tungstophosphoric species is a suitable catalyst for the esterification of free fatty acids, and in our case, this heteropolyacid retains its catalytic activity upon immobilization over the zirconia with no substantial modifications but for a slight increase in the conversions due to a synergistic effect with the low-to-moderately active support. According to our studies, the catalyst with a heteropolyacid loading of 30 wt.% is the most efficient in the esterification of palmitic acid with methanol at 60 °C because it constitutes the sample with the lower loss of catalytic activity over successive reaction runs among all of the materials prepared in this work. The amount of heteropolyacid leached from our catalysts toward the reaction medium is much lower than that observed for other supported catalysts based on the 12-tungstophosphoric species, but nevertheless, the materials prepared in this work do undergo some fouling and subsequent loss of activity due to the retention of organic matter in the microporous structure with partial blocking of the porosity.

Acknowledgements

Appendix A. Supplementary data

Supplementary data associated with this article can be found, in the online version, at http://dx.doi.org/10.1016/j.apcatb.2017.10.066.

References

[1] I. Noshadi, N.A.S. Amin, R.S. Parnas, Fuel 94 (2012) 156–164.
[2] C. Posten, G. Schaub, J. Biotechnol. 142 (2009) 64–69.
[3] M.K. Lam, K.T. Lee, A.R. Mohamed, Biotechnol. Adv. 28 (2010) 500–518.
[4] D.Y.C. Leung, X. Wu, M.K.H. Leung, Appl. Energy 87 (2010) 1083–1095.
[5] Z. Helwani, M.R. Othman, N. Aziz, J. Kim, W.J.N. Fernando, Appl. Catal. A 363 (2009) 1–10.
[6] M. Canakci, Bioresour. Technol. 98 (2007) 183–190.
[7] N.A. Zafiropoulos, H.L. Ngo, T.A. Foglia, E.T. Samulski, W. Lin, Chem. Commun. (2007) 3670–3672.
[8] A.A. Apostolakou, I.K. Kookos, C. Marazioti, K.C. Angelopoulos, Fuel Process. Technol. 90 (2009) 1023–1031.
[9] M. Canakci, J. Van Gerpen, Trans. ASAE 44 (2001) 1429–1436.
[10] J.M. Marchetti, V.U. Miguel, A.F. Errazu, Fuel 86 (2007) 906–910.
[11] M.E. Borges, L. Díaz, Renew. Sustain. Energy Rev. 16 (2012) 2839–2849.
[12] S.B. Neji, M. Trabelsi, M.H. Frikha, Energies 2 (2009) 1107–1117.
[13] L. Xu, Y. Wang, X. Yang, X. Yu, Y. Guo, J.H. Clark, Green Chem. 10 (2008) 746–755.
[14] D.E. López, J.G. Goodwin Jr., D.A. Bruce, S. Furuta, Appl. Catal. A 339 (2008) 76–83.
[15] G.D. Yadav, A.D. Murkute, J. Catal. 224 (2004) 218–223.
[16] P.S. Sreeprasanth, R. Srivastava, D. Srinivas, P. Ratnasamy, Appl. Catal. A 314 (2006) 148–159.
[17] (a) M.T. Pope, A. Müller, Angew. Chem. Int. Ed. Engl. 30 (1991) 34–48;
(b) M.T. Pope, A. Müller (Eds.), Polyoxometalates: from Platonic Solids to Antiretroviral Activity, Kluwer Academic Publishers, Dordrecht, The Netherlands, 1994;
(c) M.T. Pope, A. Müller (Eds.), Polyoxometalate Chemistry: from Topology via Self-Assembly to Applications, Kluwer Academic Publishers, Dordrecht, The Netherlands, 2001;
(d) T. Yamase, M.T. Pope (Eds.), Polyoxometalate Chemistry for Nano-Composite Design, Kluwer Academic/Plenum Publishers, New York NY, USA, 2002;
(e) F. Sécheresse (Ed.), Polyoxometalate Chemistry: Some Recent Trends, World Scientific, Singapore, 2013.
[18] (a) I.V. Kozhevnikov, Catalysts for fine chemical synthesis, Catalysis by Polyoxometalates vol. 2, John Wiley & Sons, Chichester, UK, 2002;
(b) J.B. Moffat, Metal-Oxygen Clusters: The Surface and Catalytic Properties of Heteropoly Oxometalates, Springer Heidelberg, Germany, 2001.
[19] J.B. Moffat, Metal-Oxygen Clusters: The Surface and Catalytic Properties of Heteropoly Oxometalates, Kluwer Academic/Plenum Publishers, New York NY, USA, 2001.
[20] R.A. Sheldon, R.S. Downing, Appl. Catal. A 189 (1999) 163–183.
[21] J. Alcañiz-Monge, G. Trautwein, S. Parres-Esclapez, J.A. Maciá-Agulló, Microporous Mesoporous Mat. 115 (2008) 440–446.
[22] A.I. Tropecêlo, M.H. Casimiro, I.M. Fonseca, A.M. Ramos, J. Vital, J.E. Castanheiro, Appl. Catal. A 390 (2010) 183–189.
[23] C.F. Oliveira, L.M. Dezaneti, F.A.C. Garcia, J.L. de Macedo, J.A. Dias, S.C.L. Dias, K.S.P. Alvim, Appl. Catal. A 372 (2010) 153–161.
[24] J. Alcañiz-Monge, G. Trautwein, J.P. Marco-Lozar, Appl. Catal A 468 (2013) 432–441.
[25] A.K. Endalew, Y. Kiros, R. Zanzi, Biomass Bioenergy 35 (2011) 3787–3809.
[26] M. Mittelbach, C. Remschmidt, M. Mittelbach (Ed.), Biodiesel The Comprehensive Handbook, third ed., Martib Mittelbach Publisher, Graz, Austria, 2006.
[27] A. Srivastava, R. Prasad, Renew. Sustain. Energy Rev. 4 (2000) 111–133.
[28] S. Brunauer, P.H. Emmett, E. Teller, J. Am. Chem. Soc. 60 (1938) 309–319.
[29] M.M. Dubinin, Porous structure and adsorption properties of active carbons, in: P.L. Walker (Ed.), Chemistry and Physics of Carbon, vol. 2, Marcel Dekker, New York NY, USA, 1966, pp. 51–120.
[30] D. Cazorla-Amorós, J. Alcañiz-Monge, A. Linares-Solano, Langmuir 12 (1996) 2820–2824.
[31] M. Thommes, K. Kaneko, A.V. Neimark, J.P. Olivier, F. Rodriguez-Reinoso, J. Rouquerol, K.S.W. Sing, Pure Appl. Chem. 87 (2015) 1051–1069.
[32] I.K. Song, J.R. Kitchin, M.A. Barteau, Proc. Natl. Acad. Sci. U. S. A. 99 (2002) 6471–6475.
[33] S. Farhadi, M. Zaidi, Appl. Catal. A 354 (2009) 119–126.
[34] Y. Yang, Q. Wu, Y. Guo, C. Hu, E. Wang, J. Mol. Catal. A: Chem. 225 (2005) 203–212.
[35] K. Byrappa, T. Adschiri, Prog. Cryst. Growth Charact. Mater. 53 (2007) 117–166.
[36] JCPDS 80-2155C.
[37] JCPDS 7-3430M.
[38] C.S. Cundy, P.A. Cox, Chem. Rev. 103 (2003) 663–702.
[39] M.J. Janik, R.J. Davis, M. Neurock, J. Phys. Chem. B 108 (2004) 12292–12300.
[40] B. El Bakkali, Catalizadores Heterogéneos Basados en Polioxometalatos: Aplicaciones en Reacciones de Interés Industrial y Medioambiental, Ph.D. Thesis, Available online at http://hdl.handle.net/10045/54709 (last Accessed 11 October 2017) Universidad de Alicante, Alicante, Spain, 2016.
[41] J.M. Hernández Enríquez, L.A. Cortez Lajas, R. García Alamilla, A. Castillo Mares, G. Sandoval Robles, L.A. García Serrano, J. Alloys Compd. 483 (2009) 425–428.
[42] S. Patel, N. Purohit, A. Patel, J. Mol. Catal. A: Chem. 192 (2003) 195–202.
[43] J. Arichi, M. Eternot, B. Louis, Catal. Today 138 (2008) 117–122.
[44] S. Shinachi, M. Matsushita, K. Yamaguchi, N. Mizuno, J. Catal. 233 (2005) 81–89.
[45] G. Mestl, T. Ilkenhans, D. Spielbauer, M. Dieterle, O. Timpe, J. Kröhnert, F. Jentoft, H. Knözinger, R. Schlögl, Appl. Catal. A 210 (2001) 13–34.
[46] J. Zhao, W. Fan, D. Wu, Y. Sun, J. Non-Cryst. Solids 261 (2000) 15–20.
[47] D. Jin, Z. Hou, Y. Luo, X. Zheng, J. Mol. Catal. A: Chem. 243 (2006) 233–238.
[48] M.A. Schwegler, M. van der Eijk, H. van Bekkum, Appl. Catal. A 80 (1992) 41–57.
[49] G. Sunita, B.M. Devassy, A. Vinu, D.P. Sawant, V.V. Balasubramanian, S.B. Halligudi, Catal. Commun. 9 (2008) 696–702.
[50] J.A. Melero, J. Iglesias, G. Morales, Green Chem. 11 (2009) 1285–1308.
[51] S.K. Das, S.A. El-Safty, ChemCatChem 5 (2013) 3050–3059.
[52] G. Ertl, H. Knözinger, F. Schüth, Handbook of Heterogeneous Catalysis, in: J. Weitkamp (Ed.), 2nd edition, Wiley/VCH, Weinheim, Germany, 2008.
[53] L.R. Pizzio, P.G. Vázquez, C.V. Cáceres, M.N. Blanco, Appl. Catal. A 256 (2003) 125–139.
[54] Y. Liu, E. Lotero, J.G. Goodwin Jr., J. Catal. 243 (2006) 221–228.